A 3.4mW 65nm CMOS 5^{th} Order Programmable Active-RC Channel Select Filter for LTE Receivers

Mohammed Abdulaziz, Anders Nejdel, Markus Törmänen and Henrik Sjöland
Lund University, Lund, Sweden

***Abstract*—In this work a low power 5^{th} order chebyshev active-RC low pass filter that meets Rel-8 LTE receiver requirements has been designed with programmable bandwidth and overshoot. Designed for a homodyne LTE receiver, filter bandwidths from 700kHz to 10MHz are supported. The bandwidth of the operational amplifiers is improved using a novel phase enhancement technique. The filter was implemented in 65nm CMOS technology with a core area of 0.29mm^2. Its total current consumption is 2.83mA from a 1.2V supply. The measured input referred noise is 39nV/$\sqrt{\text{Hz}}$, the in-band IIP3 is 21.5dBm, at the band-edge the IIP3 is 20.7dBm, the out-of-band IIP3 is 20.6dBm, and the compression point is 0dBm.**

***Index Terms*—Active filters, low pass filters, low power electronics, CMOS technology, Operational Amplifiers.**

I. Introduction

Wireless communication standards such as LTE with high data rates require receivers with wide band channel select filters. Moreover, these filters must have high dynamic range to be able to reject strong interference while receiving weak signals. It is also required that different filter parameters like the bandwidth can be tuned digitally. Architectures of choice for such high performance filters for wireless applications is usually g_m-C or active-RC.

Although g_m-C filters have the advantage of high bandwidth and low noise, they suffer from poor linearity due to open loop operation, nonetheless they are superior for high frequency applications [1]. In contrast, active-RC filters have high dynamic range due to closed loop operation, but can not operate at as high frequencies as their g_m-C counterparts. The reason is that the operational amplifiers (OPAMPs) must have a gain bandwidth product (GBP) that by far exceeds the filter cut-off frequency. They must also provide sufficient low frequency loop gain, and the demanding requirements result in high OPAMP power consumption [2].

In this paper a low power 5^{th} order low pass active-RC filter is presented. The power dissipated by the filter is reduced by using a new phase enhancement technique that improves both the 3-dB bandwidth and the GBP while controlling the phase margin. Also the common mode feedback (CMFB) stability is improved. The filter supports all Rel-8 LTE bands [3] with $\pm$ 40% of tuning range to counter process variations.

This paper will start by presenting the OPAMP architecture and compensation in Section II, and then the filter architecture in Section III. This is followed by measurement results and comparison with State-of-The-Art designs in Section IV, and conclusions in Section V.

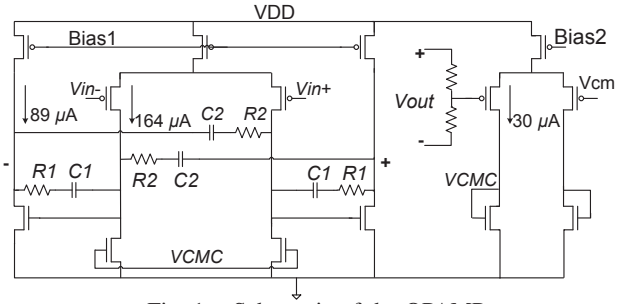

Fig. 1. Schematic of the OPAMP.

II. The Amplifier Design

Representing the active part, the OPAMP is the main building block of the filter. We use the well-known differential two stage topology with CMFB, Fig. 1. The OPAMP consumes 0.56mA from a 1.2V supply. Of this 0.328mA is used in the input stage to improve the noise performance.

Using conventional multi-stage Miller pole splitting compensation, the 3-dB bandwidth and GBP get heavily decreased in order to improve the phase margin. Compensation improvement attempts have been reported successful in improving the 3-dB bandwidth, however, GBP is not improved and the phase margin gets reduced as the poles become complex conjugate[4], [5].

In this work we propose a phase enhancement technique (see Fig. 1), where two zeros are introduced in the numerator from the negative and positive feedback resistor-capacitor links. At the same time a forth pole that is located above the transition frequency of the OPAMP is introduced by the positive feedback.

The main idea is to use the two zeros to cancel two of the dominant poles. This leaves one dominant pole pushed high enough in frequency and another one that is outside the range of operation. Ultimately we get a two-stage single pole OPAMP, and as a result both the 3-dB bandwidth and the GBP increase significantly while having the required phase margin.

The small signal half circuit of the fully differential topology is shown in Fig. 2, where C_{par1} is the lumped parasitic capacitance at the input of the second stage, r_{o1} and r_{o2} the output resistances of the first and the second stage, respectively, g_m is the transconductance of the second stage, and C_L is the load.

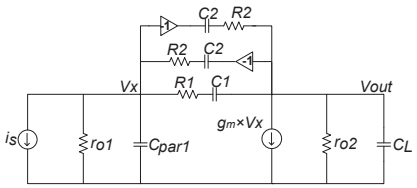

Fig. 2. A conceptual small signal model of the OPAMP.

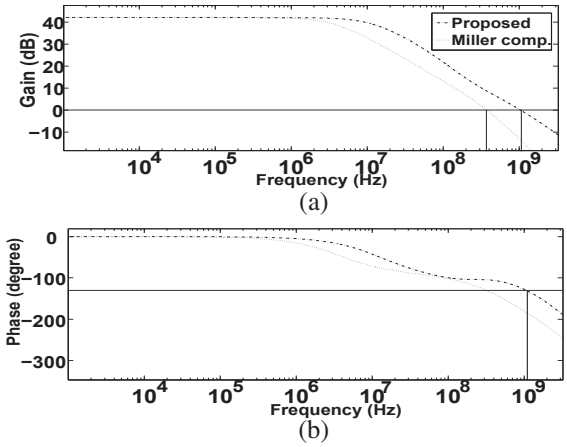

Fig. 3. Frequency response for the Miller and the proposed compensation (a) gain and bandwidth and (b) Phase margin.

It is easy to see in Fig. 2 that the DC gain of the OPAMP is unchanged. The values of the passive components can be chosen in different ways. A recommended approach is to choose equal capacitor sizes $C_1 = C_2 = C$ to make the term $g_m r_{o1} r_{o2}$ disappear from the equation of the first pole. The capacitor value should be small to improve the slew rate and frequency performance and to minimize the area. As for the resistors we choose two values close enough to assume the term $(R_1 - R_2) g_m r_{o1} r_{o2}$ negligible in the second pole and push the pole higher in frequency. Under the mentioned assumptions very simplified equations for the zeros and poles of the OPAMP are shown in (1) to (6).

Looking at (3) we see that the first pole is located high in frequency compared to the conventional Miller compensation. The second pole (4) can be canceled by tuning the first zero (1) with R_1 and R_2. The second zero (2) can be equated with the third pole, and we are left with the forth pole that is located high in frequency since C_{par1} is small.

It must emphasized that the equations (1) to (6) are approximations and that more detailed equations must be used to find more accurate pole and zero positions. Unfortunately these equations are complicated and due to the limited space available the full equations can not be presented in this paper.

Simulating the OPAMP using the conventional Miller compensation in comparison to the phase enhancement technique shows an improvement of more than three times

TABLE I
PERFORMANCE OF DIFFERENT OPAMP COMPENSATION TECHNIQUES

	Miller Comp.	**Phase Enhancement**
3-dB Bandwidth (MHz)	3.67	11.83
GBP (MHz)	378	1050
Phase Margin (°)	43.2	50.7

TABLE II
CORNER SIMULATIONS OF THE OPAMP WITH PHASE ENHANCEMENT

	FF	**TT**	**SS**	**FS**
3-dB Bandwidth (MHz)	15.22	11.83	9.026	8.4
GBP (MHz)	1302	1050	703	530
Phase Margin (°)	52.8	50.7	53.5	63.5

$$Z_1 \approx \frac{1}{C(R_1 + R_2)} \tag{1}$$

$$Z_2 \approx \frac{R_1 + R_2}{C(R_1 R_2)} \tag{2}$$

$$P_1 \approx \frac{1}{(C_L + 2C) ro2 + 2C ro1} \tag{3}$$

$$P_2 \approx \frac{(C_L + 2C) ro2 + 2C ro1}{2C_L C ro1 ro2 + C^2 (4 ro1 ro2)} \tag{4}$$

$$P_3 \approx \frac{2C_L + 4C}{C_L C (R_1 + R_2)} \tag{5}$$

$$P_4 \approx \frac{R_1 + R_2}{C_{par1} R_1 R_2} \tag{6}$$

in the 3-dB bandwidth and about three times in GBP for the same power consumption, see Table I and Fig. 3. At the same time the phase margin is 7° higher than when using Miller compensation, i.e. the improvement is even larger if we target the same phase margin. Moreover, simulations of different process corners, Fast-Fast (FF), Typical-Typical (TT), Slow-Slow (SS), and Fast-Slow (FS) show that the phase margin is maintained over process variations, Table II. Added to that, changing the temperature by ± 30 °C from room temperature changes the phase margin by no more than ± 5°. The proposed phase enhancement compensation is robust to process and temperature variations, since unlike Miller compensation the pole locations are independent of g_m. The phase margin is mainly determined by the compensation resistor-capacitor links and C_L. In Monte Carlo simulation (1000 runs) the phase margin is varying by just ±1° for 95% of the runs, and also simulations of different corners with the values of R1 and R2 set to the maximum and minimum expected values indicate similar robustness. Furthermore, step response simulation of the complete filter at different corners indicates that the filter performance is not affected by the process corner.

It is concluded that the proposed compensation tech-

nique improves the overall OPAMP frequency response, and even silicon area, without any significant compromise. It is also very robust to temperature and process variations. All of this has major benefits in filter design, allowing power efficient high dynamic range filters with increased bandwidth to be designed.

III. Filter Design

A 5^{th} order low pass chebyshev filter was implemented to provide sufficient attenuation of out of band interference. The pass band ripple is 1.5dB worst case in the 10MHz bandwidth, below 1dB for the 7.5MHz bandwidth, and less than 0.4dB for the other bandwidths in use. The architecture of the filter is leapfrog (Fig. 4) which simulates the I-V relations of an LC filter prototype. The leapfrog architecture was chosen because it is robust against component spread (mismatch). It is also easy to tune parameters like filter bandwidth and gain as they have a linear relation to the resistor and capacitor values [2].

The filter supports all Rel-8 LTE bandwidths, namely, 10MHz, 7.5MHz, 5MHz, 2.5MHz, 1.5MHz and 0.7MHz. (The RF bandwidths are two times the filter bandwidths in a homodyne receiver). The switching between bandwidths is performed using a bank of switched capacitors. To account for process, voltage and temperature variations, 5-bit unit cell based resistor banks were used, providing a tuning range of $\pm$ 40%.

All of the capacitor and resistor bank switches were located at the input (virtual ground) side of the OPAMP. The associated parasitic capacitance reduces the frequency of the pole of the input node, decreasing the phase margin of the system, resulting in overshoot at the band edge [6]. Smaller switches would solve the problem, but the linearity performance would be severely harmed. To address the overshoot problem, the technique introduced in [6] (Q-Tuning) is instead used here, where a variable resistor bank is used in series with the capacitor bank, see Fig. 4.

The filter has a digital interface to control the operating bandwidth, the bandwidth fine tuning, and also the Q-tuning. This makes it possible to control the filter operation through a digital signal processor (DSP), which becomes more attractive as the technology scales down and DSP implementations become lower and lower in cost.

IV. Measurement Results

A filter prototype was designed and fabricated in 65nm CMOS technology, see chip photo in Fig. 5. The core area is 0.29mm^2, excluding the pads and output buffers. In all measurements the total filter current consumption is 2.83mA from a 1.2V supply.

The measurement setup is shown in Fig. 6, where the baluns (ZFSCJ-2-2) are used to enable usage of single-ended equipment. Low noise external buffers (B1, B2) are used to drive the 50Ω instrument. To drive these external buffers an on-chip OPAMP-based buffer (BUF) is used and its linearity degradation is de-embedded from the measurements.

TABLE III
Comparison with Other Works

Parameter	[6]	[7]	[8]	This Work
Technology (nm)	130	90	180	**65**
Filter Type	Cheb.	Butter.	Butter.	**Cheb.**
Area (mm^2)	0.2	0.239	0.23	**0.29**
Order	5^{th}	6^{th}	3^{rd}	**5^{th}**
Supply (V)	1.5	1	1.2	**1.2**
Power (mW)	11.25	4.35	11.1	**3.4**
$\mathbf{f_{cutoff}}$ (MHz)	8.9,19.7	8.1,13.5	0.5,20	**0.44,14**
IIP3 (dBm)in-	18.3	22.1	19	**21.5**
,out-of-band	,-	,18.9	,13	**,20.6**
Noise (nV/$\sqrt{\text{Hz}}$)	30	75	12	**38.75**
SFDR	55.2	54.4	60.9	**56.8**
FoM (fJ)	0.35	0.268	0.15	**0.100**

The frequency response for each bandwidth is shown in Fig. 7. The losses of the test setup and the output buffers have been de-embedded. The gain variation over bandwidth tuning is about 1dB (approx. from 5.2dB to 4.2dB).

Q-tuning was implemented to control overshoot resulting from the parasitic pole at the input of the OPAMPs or from low temperature operation. Fig. 8 shows the Q-tuning steps which range from high overshoot to the over-compensated state to account for all possible environment conditions.

To estimate the dynamic range a two tone test (1MHz,1.1MHz tones for the in-band and 22.5MHz,40MHz for out-of-band) was performed to measure IIP3. The in-band-IIP3 is found to be 21.5dBm, the out-of-band is 20.6dBm, at the band edge the IIP3 is 20.7dBm and the achieved Compression Point (CP) is 0dBm. The measured average input referred noise floor is just 39nV/$\sqrt{\text{Hz}}$ and the integrated noise from 20Hz to 10MHz is 122μV_{rms}. With these measurement results the commonly used Figure of Merit (FoM) shown in (7) can be calculated.

$$FoM = \frac{Power}{Order \cdot SFDR \cdot Bandwidth} \tag{7}$$

Where SFDR is the Spurious Free Dynamic Range and it is given by: $\frac{2}{3}(IIP_3 - P_{noise})$.

The performance summary and comparison with some previous works is shown in Table III. It can be seen that the power consumption is reduced compared to other works. The area is slightly larger, but this work supports much lower cut-off frequencies than the works[7], [6].

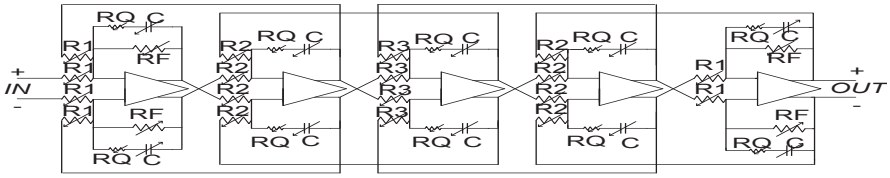

Fig. 4. 5^{th} order filter schematic.

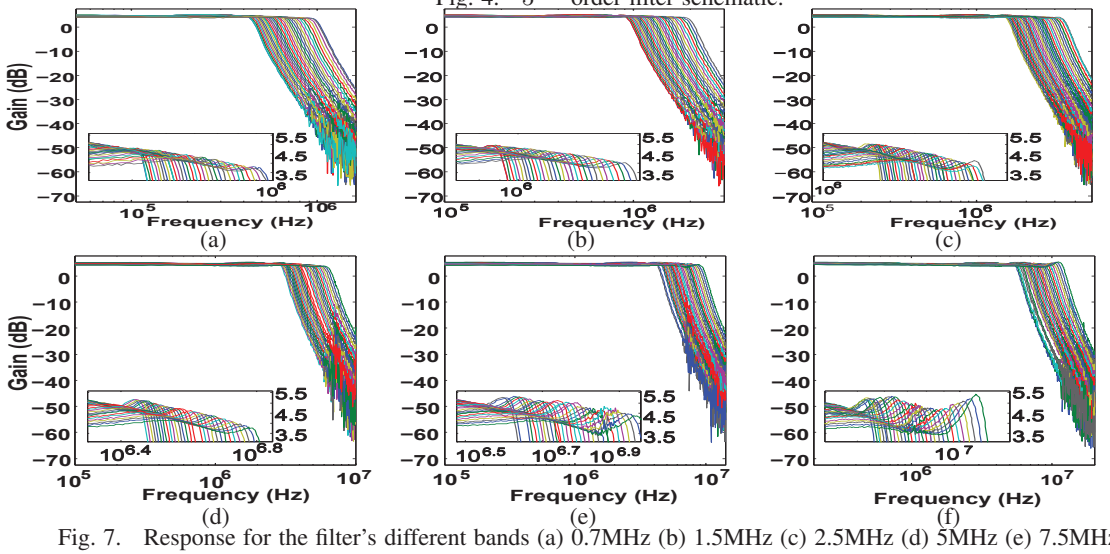

Fig. 7. Response for the filter's different bands (a) 0.7MHz (b) 1.5MHz (c) 2.5MHz (d) 5MHz (e) 7.5MHz (f) 10MHz

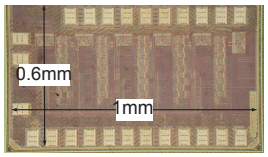

Fig. 5. Chip photo.

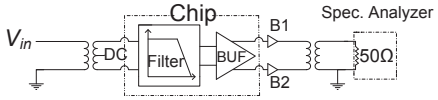

Fig. 6. Measurement setup.

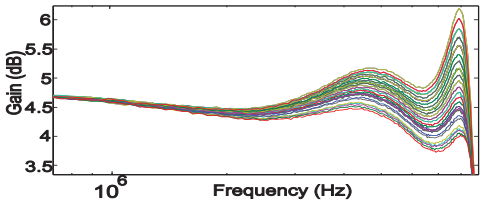

Fig. 8. Q-tuning different steps.

V. Conclusion

A low power 5^{th} order active-RC filter for Rel-8 LTE receivers has been fabricated in 65nm CMOS and measured. The OPAMP in the filter benefits from a novel compensation technique that significantly improves its performance. Simulations and measurements prove the technique to be power efficient and robust to process and temperature variations. The filter measurement results show high dynamic range combined with wide range bandwidth tuning and Q-tuning to compensate for all possible operation scenarios.

Acknowledgment

The authors would like to thank Swedish Foundation for Strategic Research (SSF) for funding the Digitally-Assisted Radio Evolution (DARE) project, and ST-Microelectronics for fabrication of the chip.

References

[1] T. Lo *et al.*, *1V CMOS $G_m - C$ Filters*. Springer, 2009.

[2] R. Schaumann *et al.*, *Design of Analog Filters*. OXFORD University Press, 2010.

[3] U. E. radio transmission and reception. (2009) 3GPP TS 36.101, 3GPP specifications. [Online]. Available: http://www.3gpp.org

[4] M. Vadipour, "Capacitive feedback technique for wide-band amplifiers," *IEEE Journal of Solid-State Circuits*, vol. 28, no. 1, pp. 90 –92, Jan. 1993.

[5] A. Vasilopoulos *et al.*, "A Low-Power Wideband Reconfigurable Integrated Active-RC Filter With 73 dB SFDR," *IEEE Journal of Solid-State Circuits*, vol. 41, no. 9, pp. 1997 – 2008, Sept. 2006.

[6] S. Kousai *et al.*, "A 19.7 MHz, Fifth-Order Active-RC Chebyshev LPF for Draft IEEE802.11n With Automatic Quality-Factor Tuning Scheme," *IEEE Journal of Solid-State Circuits*, vol. 42, no. 11, pp. 2326 –2337, Nov. 2007.

[7] M. Oskooei *et al.*, "A CMOS 4.35-mW +22-dBm IIP3 Continuously Tunable Channel Select Filter for WLAN/WiMAX Receivers," *IEEE Journal of Solid-State Circuits*, vol. 46, no. 6, pp. 1382 –1391, June 2011.

[8] T.-Y. Lo *et al.*, "A Wide Tuning Range Gm-C Filter for Multi-Mode CMOS Direct-Conversion Wireless Receivers," *IEEE Journal of Solid-State Circuits*, vol. 44, no. 9, pp. 2515 –2524, Sept. 2009.